Identification of TNFRSF1A as a potential biomarker for osteosarcoma

Yuke Zhang[a,1], Kai Liu[a,1] and Jianzhong Wang[b,*]

[a]*Inner Mongolia Medical University, Hohhot, Inner Mongolia, China*
[b]*Department of Orthopedics and Traumatology, The Second Affiliated Hospital of Inner Mongolia Medical University, Hohhot, Inner Mongolia, China*

Abstract.

BACKGROUND: Osteosarcoma (OS) is a relatively rare malignant bone tumor in teenagers; however, its molecular mechanisms are not yet understood comprehensively.

OBJECTIVE: The study aimed to use necroptosis-related genes (NRGs) and their relationships with immune-related genes to construct a prognostic signature for OS.

METHODS: TARGET-OS was used as the training dataset, and GSE 16091 and GSE 21257 were used as the validation datasets. Univariate regression, survival analysis, and Kaplan-Meier curves were used to screen for hub genes. The immune-related targets were screened using immune infiltration assays and immune checkpoints. The results were validated using nomogram and decision curve analyses (DCA).

RESULTS: Using univariate Cox regression analysis, TNFRSF1A was screened from 14 NRGs as an OS prognostic signature. Functional enrichment was analyzed based on the median expression of TNFRSF1A. The prognosis of the TNFRSF1A low-expression group in the Kaplan-Meier curve was notably worse. Immunohistochemistry analysis showed that the number of activated T cells and tumor purity increased considerably. Furthermore, the immune checkpoint lymphocyte activation gene 3 (LAG-3) is a possible target for intervention. The nomogram accurately predicted 1-, 3-, and 5-year survival rates. DCA validated the model (C = 0.669).

Conclusion: TNFRSF1A can be used to elucidate the potential relationship between the immune microenvironment and NRGs in OS pathogenesis.

Keywords: Osteosarcoma, necroptosis, tumor immune microenvironment, TNFRSF1A, prognosis

1. Introduction

Osteosarcoma, a prevalent bone tumor, predominantly affects adolescents, with the disease typically manifesting between the ages of 15–20 [1]. This neoplasm exhibits a bimodal age distribution, featuring a secondary peak in incidence among individuals aged 65 and above [2]. In the year 2000, the mortality rate for osteosarcoma was 0.021 per 100,000 individuals, escalating to a peak of 0.132 per 100,000 individuals in 2018 [3]. Notably, the elderly subgroup manifests the lowest five-year survival rate, likely attributable to concurrent non-neoplastic complications [3]. Over the past two decades, the 5-year survival rate has shown improvement, reaching 60–70% in patients with localized tumors. However, for patients with recurrent or metastatic osteosarcoma, the 5-year survival rate remains below 25% [4]. Presently, early surgical intervention stands as the principal and pivotal therapeutic strategy. The administration of doxorubicin, cisplatin, and high-dose methotrexate, collectively known

---

[1]Yuke Zhang and Kai Liu contributed equally to this work and share first authorship.

*Corresponding author: Jianzhong Wang, Department of Orthopedics and Traumatology, The Second Affiliated Hospital of Inner Mongolia Medical University, Hohhot, Inner Mongolia, China. Tel.: +86 471 22576222; E-mail: wangjianzhongwj@163.com.

Table 1
Baseline patient characteristics for three datasets

	GSE16091	GSE21257	TARGET
Organism	Homo sapiens	Homo sapiens	Homo sapiens
Experiment type	Expression profiling by array	Expression profiling by array	Log2 (Count + 1)
Platforms	GPL96	GPL10295	Illumina
Sample (number)	34	53	85

as "MAP," coupled with limb-sparing surgery for primary tumor resection, is associated with an approximate 70% 5-year survival rate in cases of localized disease. In instances of distant metastasis, patients following the "MAP" treatment protocol demonstrate 5-year survival rates ranging from 10% to 40% [5]. Early diagnosis and treatment significantly enhance the prognosis of osteosarcoma. However, challenges arise due to a limited understanding of the disease's origin, leading to diagnostic difficulties and treatment delays [6]. Recent advancements in biomedicine have positioned targeted therapy as a promising avenue for osteosarcoma treatment. This involves targeted inhibition of apoptosis- [7] and autophagy-related [8] genes, combined with immunotherapy to alleviate osteosarcoma. Despite these efforts, outcomes remain unsatisfactory, underscoring the imperative for further research to elucidate the molecular mechanisms of osteosarcoma immunotherapy and identify pertinent biomarkers for immune checkpoint inhibitors.

Necroptosis, a non-cysteine protease-dependent form of cell death, exhibits morphological features identical to those of cell necrosis. However, it occurs through a distinct programmed cell death mechanism that is completely independent of the apoptosis signaling pathway [9]. Necroptosis is involved in the pathogenesis of glioblastoma [10] and non-small cell lung cancer [11] and plays an essential role in orthopedic diseases. Necroptosis inhibitors provide significant relief from osteoarthritis [12] and osteonecrosis of the femoral head [13]; therefore, necroptosis genes may also be involved in OS pathogenesis.

To date, numerous studies have analyzed pathogenesis of OS from different perspectives. Li et al. constructed a prognostic model related to autophagy in OS using univariate/multivariate Cox regression and tested the model in a validation dataset, but lacked a joint analysis of immune infiltration [14]. Hua et al. employed non-negative matrix factorization (NMF) clustering and the least absolute shrinkage and selection operator (LASSO) algorithm to identify eight necroptosis-related genes (NRGs) in OS, which were validated with a validation cohort [15]. This study provides an initial assessment of immune infiltration and the tumor microenvironment in osteosarcoma; however, it is acknowledged that incorporating research pertaining to immune checkpoints would undoubtedly enhance the comprehensive understanding of these aspects. Zheng et al. screened seven lncRNAs related to necroptosis and survival analysis showed that the lncRNAs were closely associated with poor prognosis in high-risk patients. However, the study did not use a validation dataset to test the results [16]. Although many discoveries have been made regarding OS, the mechanisms associated with NRGs in OS remain elusive.

In the present study, univariate Cox regression was used to construct a necroptosis gene-related OS model to screen for the risk gene *TNFRSF1A*. Patients with OS were classified into high- and low-risk groups using the median *TNFRSF1A* expression level as the cut-off, and survival analysis was performed for both groups. Differentially expressed genes (DEGs) and functional enrichment were analyzed. Additionally, a combined analysis of immune infiltration and immune scores was performed for the OS group. Finally, a nomogram and decision curve analysis (DCA) were performed to examine the reliability of *TNFRSF1A* in the model. Our data indicate that targeting the *TNFRSF1A* gene might enhance the therapeutic treatment of OS.

2. Materials and methods

2.1. Acquisition of gene expression data

Microarray expression profiles for OS were obtained from the Therapeutically Applicable Research to Generate Effective Treatments (TARGET) database (http://target.nci.nih.gov) [17], and microarray data from GSE16091 (GPL96) [18] and GSE21257 (GPL10295) [19] were collected from the Gene Expression Omnibus (GEO) database (https://www.ncbi.nlm.nih.gov/geo/) [20]. The three datasets were integrated using the limma package [21] and normalization within the dataset was performed using the normalizeBetweenArrays function. The TARGET-OS dataset was used as the training set, and GSE 16091 and GSE 21257 were used as the validation sets. All clinical information in the three datasets is presented in Table 1.

2.2. Selection of necroptosis genes associated with survival outcome

Univariate Cox regression analysis was conducted to screen the TARGET-OS dataset genes, with $P < 0.05$ and $SD > 0.2$. The genes were then intersected with 14 NRGs (**RIPK1, TLR2, TLR3, TLR4, TNFRSF1A, ZBP1, NR2C2, HMGB1, CXCL1, USP22, TRAF2, ALDH2, EZH2, NDRG2**) [22]. The NRG TNFRSF1A, which is more closely associated with OS survival outcomes, was obtained.

2.3. Analysis of TNFRSF1A gene expression and prognosis in the TARGET-OS cohort

The Wilcoxon test was used to examine the expression of **TNFRSF1A** in different age (older or younger than 14 years) and sex groups (female or male); box plots were drawn at the nodes, with $P < 0.05$. Survival analysis was performed using the Survival [23] and Survminer [24] packages, and Kaplan-Meier curves were plotted for the high- and low-**TNFRSF1A** expression groups in TARGET-OS.

2.4. Analysis of DEGs

The DEGs in the three datasets were analyzed based on high- and low-expression groups of **TNFRSF1A** using the Limma package. The numbers of upregulated and downregulated genes were calculated. Volcano plots and heat maps were generated using the ggplot2 and heatmap packages. DEGs from the three datasets that were clustered by hierarchical clustering were considered intersections.

2.5. Functional enrichment analysis

DEGs in TARGET-OS were analyzed and visualized for Gene Ontology (GO) [25] and Kyoto Encyclopedia of Genes and Genome (KEGG) [26] enrichment using the clusterProfiler [27,28] and GOplot packages [29], with $P < 0.05$. Gene set enrichment analysis (GSEA) [30] was performed using expression profiles from high- and low-risk groups. Gene sets of 'c5.go.v7.4. entrez.gmt' and 'c2.cp.kegg.v7.4. entrez.gmt' were obtained from the Molecular Signature Database (MSigDB) [31] for running GSEA, with $P < 0.05$.

2.6. Protein-protein interaction network of NRGs

Fourteen NRGs were used to construct PPI networks in the STRING database [32] (https://string-db.org/) with a confidence threshold of 0.4. Correlation analysis was performed for NRGs in TARGET-OS. Subsequently, a correlation heat map was plotted, and points with significance were shown in color based on correlation coefficients. Box plots of the 14 NRGs are shown for GSE16091 and GSE21257, with $P < 0.05$.

2.7. Effect of TNFRSF1A gene expression grouping on immune cell infiltration

The immune cell immunoreactive gene sets obtained from the ImmPort database (http://www.immport.org) [33] were from a previous study [34]. Correlation analysis of anti-tumor immunity and pre-tumor suppression was performed by plotting correlation scatter plots for single-sample gene set enrichment analysis (ssGSEA) [35].

2.8. Analysis of high and low TNFRSF1A expression for immunotherapy

Differences in expression at the immune checkpoints [36] were calculated for the three datasets. A violin plot was constructed using the ggplot2 package. The ESTIMATE [37] package was used to calculate stromal and immune scores, estimate scores, and determine tumor purity.

2.9. Correlation analysis of different risk factors on the prognosis of OS

The prognosis-related indicators (age and sex) for OS were selected. Age and **TNFRSF1A** expression were used as continuous variables, whereas sex was used as a categorical variable. The Forest Plot [38] package [34] was used to determine the odds ratio of each factor. The ROC curve was constructed using the pROC package and the area under the curve (AUC) was calculated. The rms package [39] generated a nomogram to predict the relationships between the variables in the model and the effectiveness of model evaluation in TARGET-OS at one, three, and five years. Prognostic performance was examined using the concordance of the index (c-index) and P-value.

2.10. Statistical analysis

To compare variables between the two groups, the Student's t-test was used for normally distributed continuous variables and the Mann-Whitney U (Wilcoxon
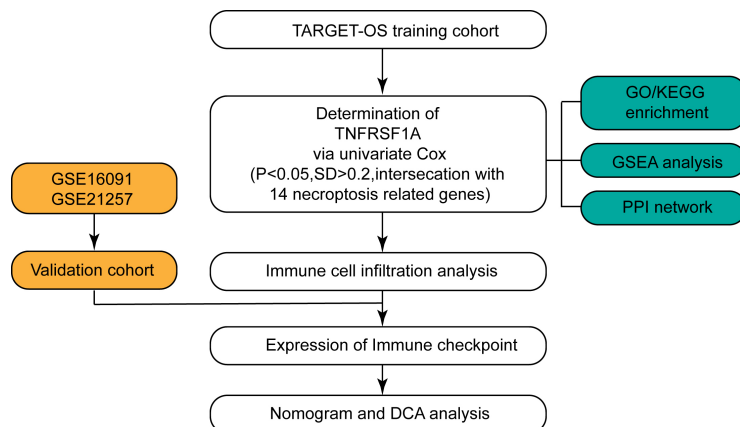
Fig. 1. Flow chart for the study. The flow chart illustrates the step-by-step workflow employed in the present study to investigate the role of TNFRSF1A in osteosarcoma development.

rank-sum) test was used for non-normally distributed continuous variables. All statistical analyses were performed in R software (https://www.r-project.org, version 4.0.2). All statistical tests were two-sided, with $P < 0.05$.

3. Results

A flowchart of the study process is shown in Fig. 1. **TNFRSF1A** was screened from the intersection of TARGET-OS and NRGs using univariate Cox regression analysis. High- and low-expression groups were distinguished based on the median expression level of **TNFRSF1A**. There were no significant differences in **TNFRSF1A** expression in the age (older or younger than 14 years) and sex (female or male) subgroups of the TARGET-OS cohort, indicating that the expression of **TNFRSF1A** was not related to age or sex in patients with OS (Fig. 2a and b). However, the survival outcomes of the high-expression groups were better than those of the low-expression groups of **TNFRSF1A** (Fig. 2c). In addition to **TNFRSF1A**, the expression of three other genes in the 14 NRGs was significantly different between the two **TNFRSF1A** risk groups (Fig. 2d): **TLR2** ($P = 0.011881$), **EZH2** ($P = 0.001441$), and **HMGB1** ($P = 0.030055$).

3.1. DEG screening

In the TARGET-OS, GSE16091, and GSE21257 datasets, DEGs were screened using the median **TNFRSF1A** expression as a cut-off and for drawing volcano plots, with absolute values of Log2FC > 0 and

$P < 0.05$, as the threshold (Fig. 3a and c). The number of upregulated genes in the three datasets was 778, 1208, and 2589, compared to 687, 2190, and 2589, respectively, for the downregulated genes. The top 10 DEGs in the three datasets were used to create a heat map to show the differences between the two **TNFRSF1A** expression groups (Fig. 3d–f). A total of 28 DEGs from the three datasets were obtained from the intersection to generate a heat map (Fig. 3g).

3.2. Enrichment analyses

A total of 1465 DEGs in the TARGET-OS dataset were analyzed using GO and KEGG enrichment analyses (Supplementary Table S1). GSEA was performed to clarify the different pathways and functions associated with different prognoses (Supplementary Table S2). Enrichment analysis primarily focuses on immune-related biological processes, including neutrophil activation, neutrophil-mediated immunity, and antigen-processing immune responses (Figs S1 and S2).

3.3. PPI network analysis for NRGs

PPI network plots were constructed using the STRING database (Fig. 4a) and the correlation coefficients of the 14 NRGs were calculated. Those with absolute values greater than 0.5 were marked with color (Fig. 4b). The expression of NRGs was calculated and plotted as a box plot between the high- and low-expression groups of TNFRSF1A (Fig. 4c and d). In GSE16091, the expression of **ALDH2** ($P = 0.0043$) and **HMGB1** ($P = 0.016$) was significantly different among the groups, whereas in GSE21257, the expres-
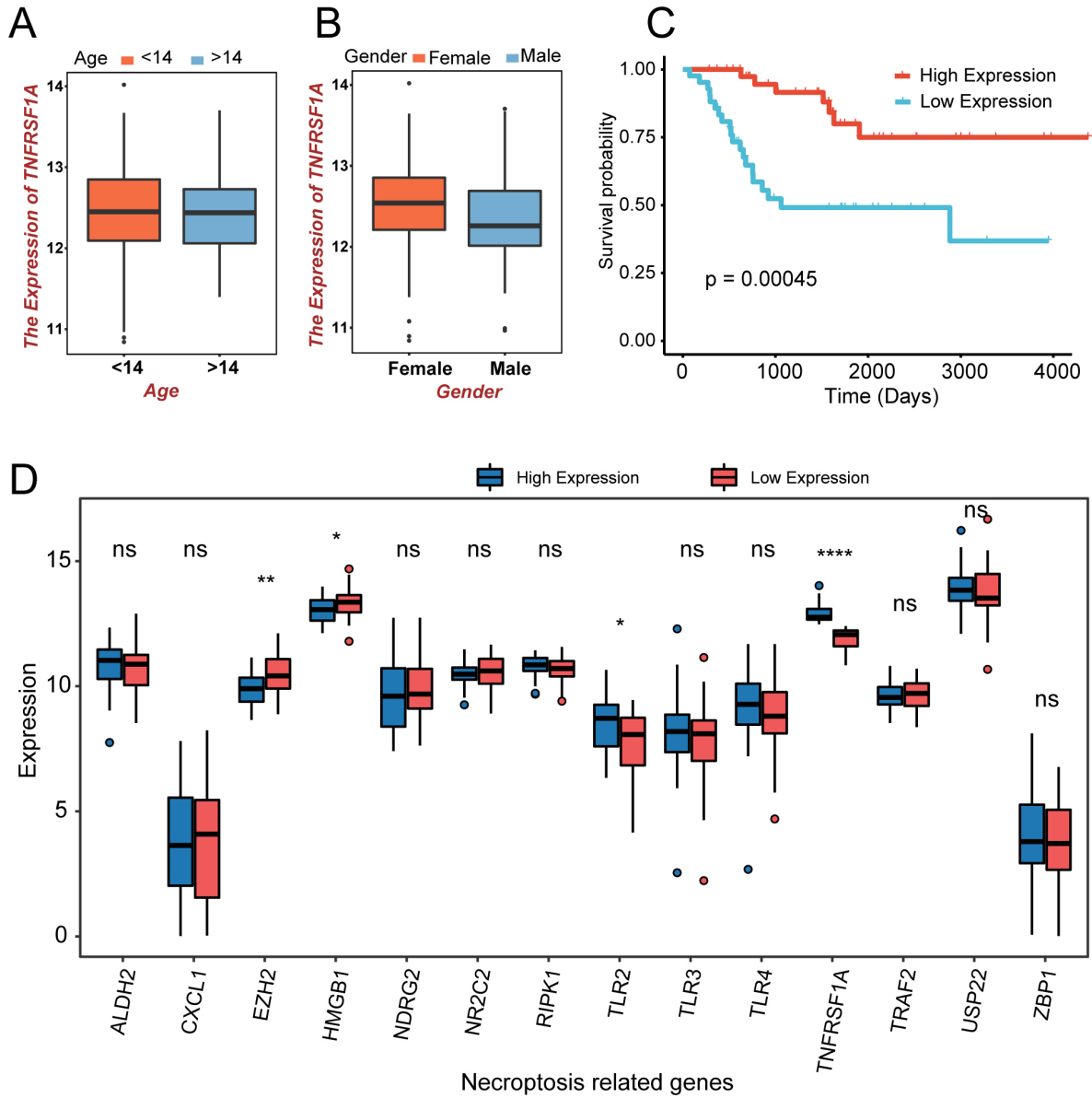
Fig. 2. The expression and prognostic analysis of NRGs in the TARGET-OS cohort. (a) Age-related expression of the TNFRSF1A gene in patients with OS; orange is less than 14 years; blue is greater than 14 years. (b) Expression of TNFRSF1A in different sexes; orange indicates males; blue indicates females. (c) K–M curve in different TNFRSF1A expression groups; orange is the high-expression group; blue is the low-expression group. (d) Box plot of NRGs expression in the two TNFRSF1A expression groups; blue is the high-expression group; red is the low-expression group. ns: $P > 0.05$, $^*P < 0.05$, $^{**}P < 0.01$, $^{****}P < 0.0001$.

sion of **TLR3** ($P = 0.006$), **TLR4** ($P = 0.045$), **ZBP1** ($P = 0.028$), **NR2C2** ($P = 0.001$), **HMGB1** ($P = 0.018$), **TRAF2** ($P = 0.003$), and **ALDH2** ($P = 0.010$) were significantly different.

3.4. Immune cell infiltration

Thedegree of immune cell enrichment was calculated using ssGSEA algorithm. The immune cell enrichment score was lower in the TNFRSF1A low-expression group than in the high-expression group (Fig. 5a). However, the correlation are weak between pro-tumor suppression and anti-tumor immunity (Fig. 5b). Immune cell infiltration analysis of Target-OS samples showed a low enrichment of type 2 T helper cells and a high enrichment of activated B cells (Fig. 5c). Box plots
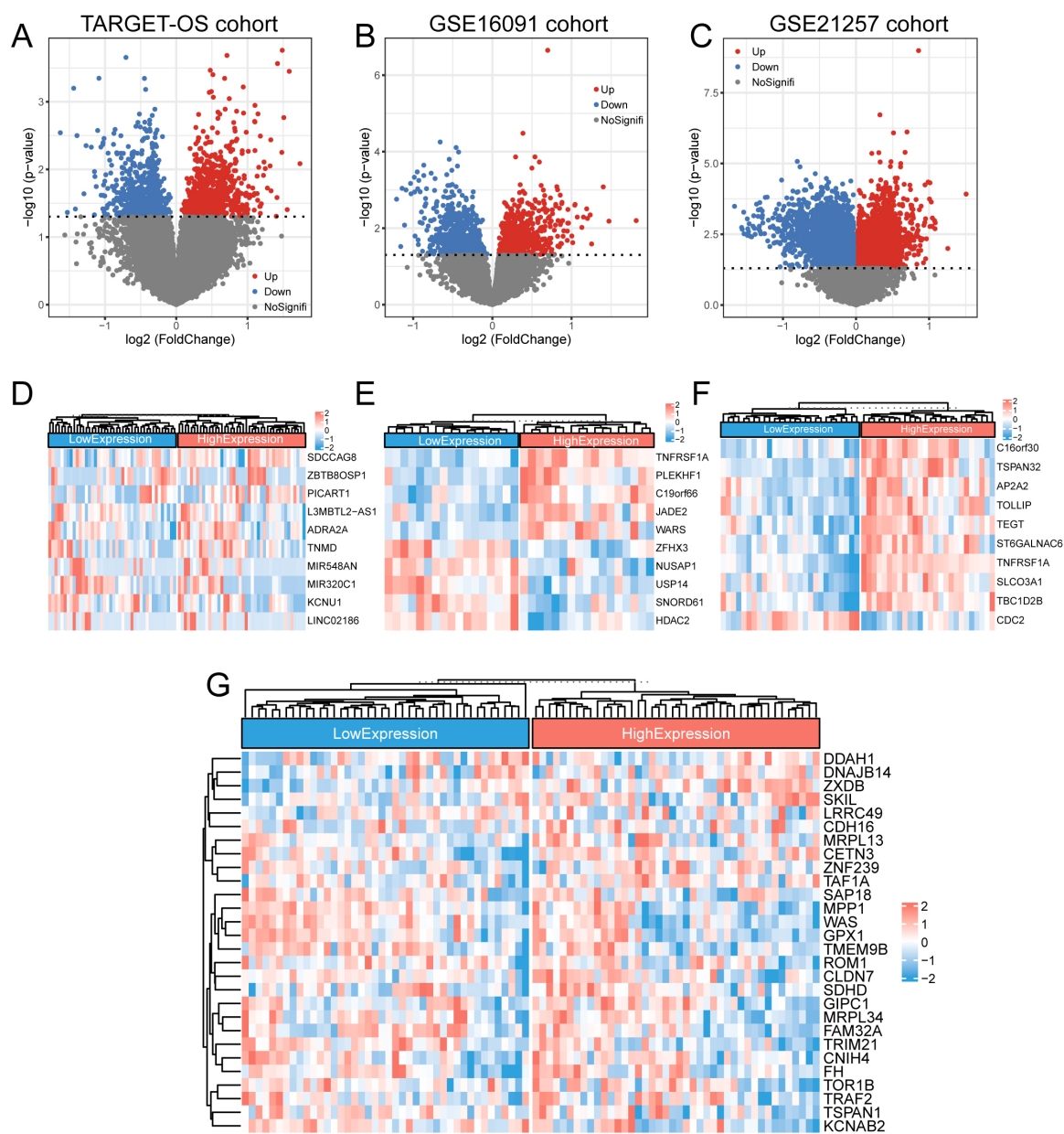
Fig. 3. DEGs in the TNFRSF1A high- and low-expression groups. (a–c) The DEGs of the TARGET-OS cohort and GSE16091 and GSE21257 datasets were screened and plotted for volcanoes, respectively, with blue representing downregulated genes and red representing upregulated genes. (d–f) Heatmaps of the top 10 DEGs in the TARGET-OS cohort and GSE16091 and GSE21257 datasets, respectively. (g) Clustered heat map of the expression profiles for the 28 DEGs common to the three datasets.

of the proportions of immune cells in the two **TN-FRSF1A** groups showed a significant difference between activated dendritic cells and activated CD8+ T cells (Fig. 5d).

3.5. Immunotherapy with immune checkpoints

The immune checkpoints Cytotoxic T lymphocyte-associated antigen-4 (**CTLA4**), lymphocyte activation gene 3 (**LAG-3**), and T cell immunoreceptor with Ig and ITIM domains (**TIGIT**) were selected to clarify the differences in immunotherapy for **TNFRSF1A**. In the TARGET-OS training set, the expression level of **LAG3** was considerably higher in the TNFRSF1A high expression group (Fig. 6a). A similar trend was evident in
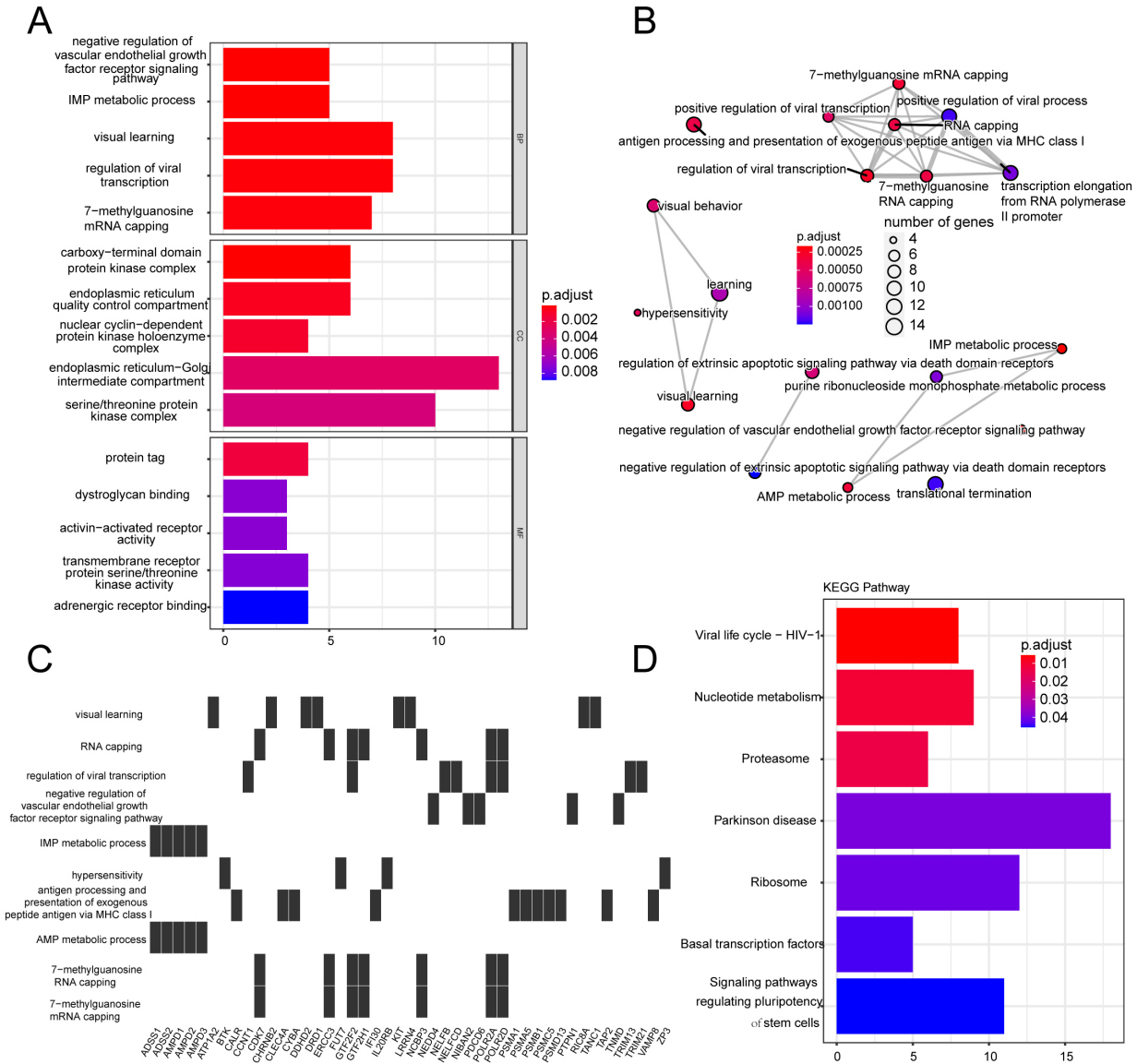
Fig. 4. PPI network analysis for NRGs. (a) PPI network plot for 14 NRGs. (b) Correlation heat map of 14 NRG expressions; points with absolute values of correlation coefficients greater than 0.5 are marked with color. Red represents positive and blue represents negative correlations. (c–d) Expression of 14 NRGs at different expression levels of TNFRSF1A in GSE16091 (c) and GSE21257 (d). ns: $P > 0.05$, *$P < 0.05$, **$P < 0.01$, ****$P < 0.0001$.

the validation dataset, GSE16091 (Fig. 6b). However, none of the three immune checkpoints was differentially expressed in the GSE21257 dataset (Fig. 6c). Stromal score, immune score, estimated score, and tumor purity were calculated using the TARGET-OS dataset. The low-expression group had lower stromal, immune, and estimated scores (Fig. 6d–f). In contrast, the tumor purity of the high-expression group was much higher (Fig. 6g).

3.6. Prognostic correlation of risk factors in OS

In the TARGET-OS dataset, a multivariate Cox regression analysis forest plot was constructed using ***TNFRSF1A*** expression, age, and sex (Fig. 7a). Only the factor "***TNFRSF1A*** expression" was located to the left of the null line (HR = 0.42, CI = 0.24–0.73, $P = 0.002$), suggesting that ***TNFRSF1A*** expression might be an important contributor to the survival outcome of patients with OS. These three factors were used as selec-
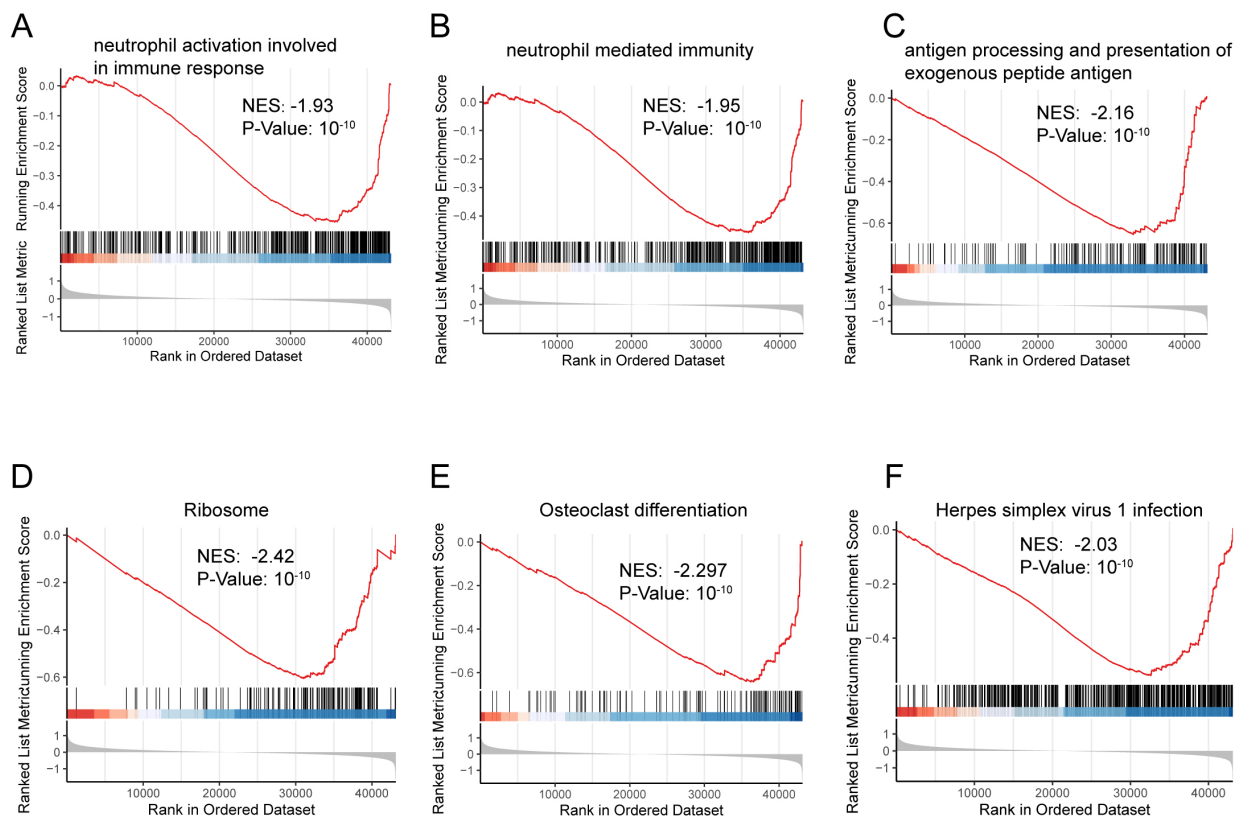
Fig. 5. Effect of TNFRSF1A expression grouping on immune cell infiltration. (a) Heat map of ssGSEA immune cell enrichment fraction. Above the first dividing line are anti-tumor cells, between the two dividing lines are pro-tumor cells, and below the second dividing line are general immune cells. (b) Scatter plot of correlation between anti-tumor immunity and pro-tumor suppression. (c) Immune cell infiltration in TARGET-OS samples. (d) Box plot of the percentage of immune cells.

tion factors for ROC curve plotting with AUC values of 0.668, 0.512, and 0.497, respectively, in the TARGET-OS cohort dataset (Fig. 7b). To evaluate the predictive ability of the model for the prognosis of patients with OS, we selected OS-related factors (***TNFRSF1A*** expression, age, and sex) to construct a nomogram to predict 1-, 3-, and 5-year survival rates (Fig. 7c). The predictive effect of the model was validated by plotting DCA curves in the TARGET-OS dataset using the RMS package to obtain the prediction results for 1-, 3-, and 5-year survival rates. Based on the fit of the curve to the gray line and C-index = 0.669, the model predicted well (Fig. 7d–f).

4. Discussion

OS, a rare malignant bone tumor, is characterized by the direct production of tumor cells in bone-like tissues, causing pathological changes in the body's bone tissue that affect bone health. Recently, owing to the

deficiency of early diagnostic markers and the rapid development of the disease, most patients with OS are already in advanced stages after diagnosis and must undergo surgery due to intolerable physical and psychological trauma [6]. In recent years, targeted gene therapy has emerged as a promising treatment for OS [8]. Necroptosis is a widely studied form of cell death, and many studies have shown that NRG can be used as a target molecule for the prognosis or diagnosis of diseases such as osteoarthritis [40] and osteoporosis [41]. However, the exact targets of NRG and its detailed therapeutic mechanisms remain unknown. In this study, ***TNFRSF1A***, a critical NRG that can be used as a diagnostic marker for OS, was screened using univariate Cox regression analysis. We used TARGET-OS as the training group, and GSE16091 and GSE21257 as the validation groups. The normality and DCA curves confirmed the validity of the model. Immune infiltration and immune checkpoint analyses performed on the three datasets indicated that ***TNFRSF1A*** is a good diagnostic marker of OS.
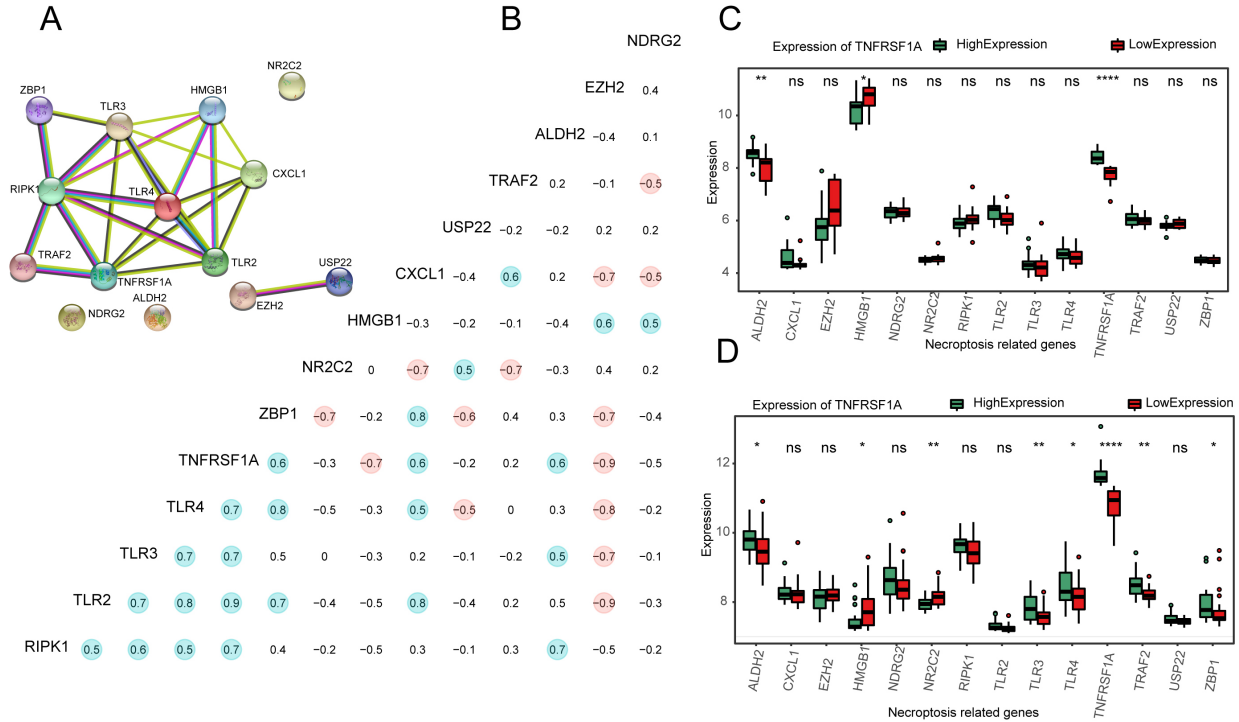
Fig. 6. Effect of TNFRSF1A expression grouping on immunotherapy in three datasets. (a–c) Expression of immune checkpoints CTLA4, LAG3, and TIGIT in the TARGET-OS cohort, GSE16091, and GSE21257 datasets. (d–g) Stromal score (d), immune score (e), estimate score (f), and tumor purity (g) were calculated using the TARGET-OS dataset in both the TNFRSF1A high- and- low-expression groups.

Necroptosis is preprogrammed death triggered by death receptors, interferons, toll-like receptors, intracellular RNA and DNA sensors, and other mediators [42]. Based on univariate Cox regression analysis, among the 14 evaluated NRGs [22], the prioritization of *TNFRSF1A* arises from its noteworthy association with OS prognosis and its pertinence in immune-related mechanisms in OS pathogenesis. The decision to investigate *TNFRSF1A* was further grounded in its established involvement in immune signaling pathways and its potential capacity to modulate tumorigenesis. Consequently, *TNFRSF1A* was designated as the central focus of subsequent endeavors involving enrichment analyses, immune analyses, and prognostic modeling. *TNFRSF1A* encodes TNF receptor type I TNFR1, also known as CD120a [43]. In addition, *TNFRSF1A* has shown potential as a biomarker for various tumors. In non-small cell lung cancer, *TNFRSF1A* is closely correlated with tumor microenvironment changes and tumor mutation burden (TMB), and is positively correlated with the adverse prognosis of the disease [44]. In clear cell renal cell carcinoma, TNFRSF1A is significantly associated with clinicopathological features, TMB, and expected survival time [45]. These results

contradict the results of the present study. However, *TNFRSF1A* acts as a protective gene involved in the regulation of pyroptosis in OS cells. In the high-risk OS group, the expression level of *TNFRSF1A* was reduced, whereas the incidence of pyroptosis was significantly increased [46]. The finding is consistent with the results of the present study. It has been suggested that *TNFRSF1A*, whether involved in necroptosis or pyroptosis, exerts an inhibitory effect on OS progression. Lung, renal, and breast cancers are visceral cancers that are mainly found in middle-aged and elderly individuals, whereas OS is more common in teenagers. Research indicates that *TNFR1* is involved in the progression of lung cancer by mediating tumor cell-induced endothelial cell death, tumor cell extravasation, and metastatic seeding [47]. *TNFR1* participates in the growth and survival of clear cell renal cell carcinoma by promoting cell cycle entry, activating NF-κB-mediated anti-apoptotic pathways, and initiating apoptotic signaling pathways [48]. Mekyt et al. found that ETS variant transcription factor 7 (**ETV7**) directly binds to intron I of the *TNFRSF1A* gene. This interaction suppresses *TNFRSF1A* protein expression, thereby impeding NF-κB signal activation and diminishing the inflammatory
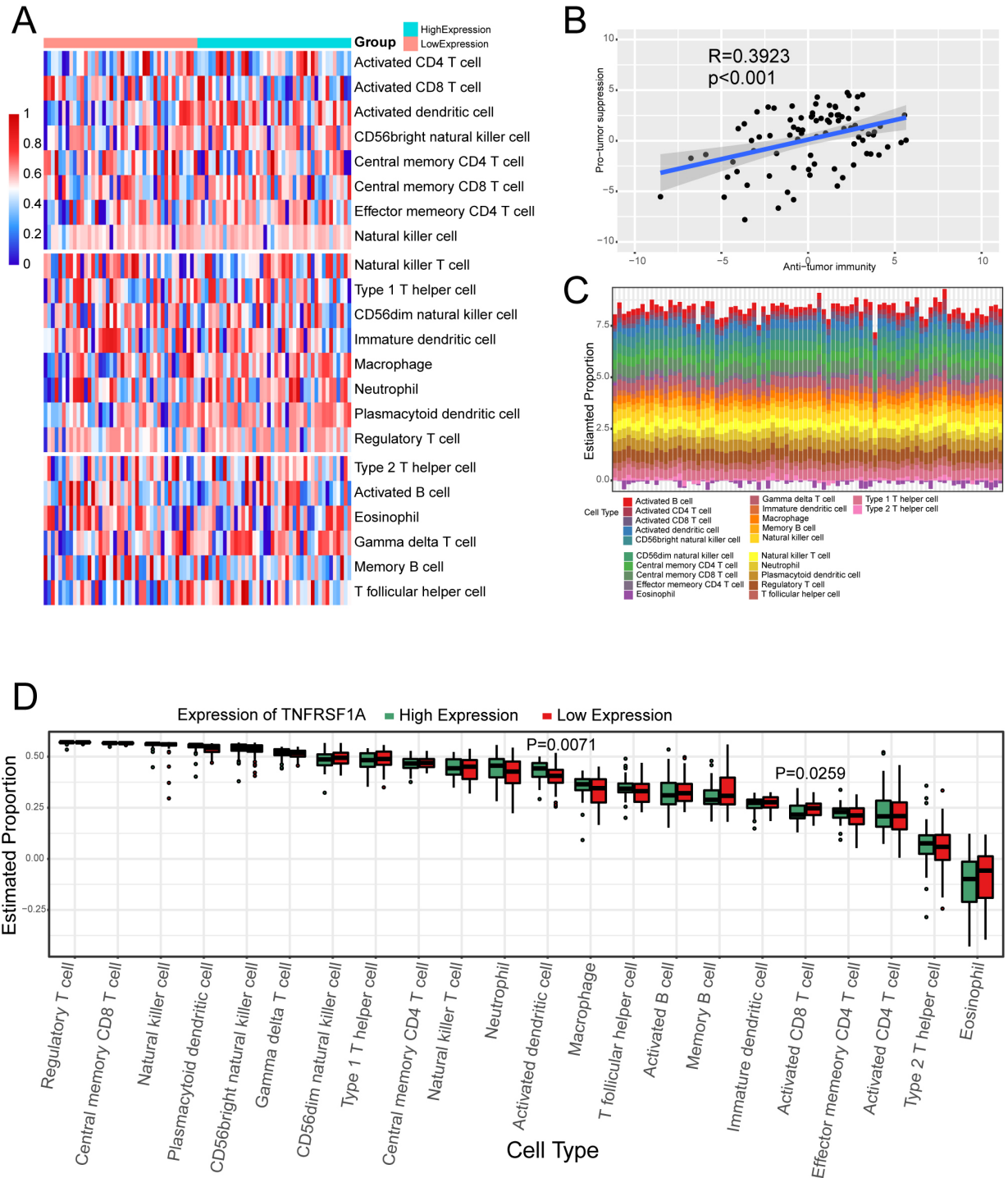
Fig. 7. Correlation analysis of different risk factors in OS prognosis. (a) Forest plot of TNFRSF1A expression, age, and sex in TARGET-OS cohort, labeled with HR and *P*-values. (b) ROC curves and AUC values of TNFRSF1A expression, age, and sex in the TARGET-OS cohort. Different colors represent different risk factors. (c) TNFRSF1A expression, age, and sex were used to construct a nomogram to predict survival of OS patients. (d–f) DCA calibration plots predicted the 1-, 3-, and 5-year survival rates of the TARGET-OS cohorts according to TNFRSF1A expression. The horizontal axis and vertical axis represent the predicted and actual survival probabilities.

response in breast cancer cells [49]. In addition, Lin et al. demonstrated that fucosyltransferase 8 (FUT8) influences OS survival by regulating the core fucosylation levels of TNF receptors (TNFRs). Decreased fucosylation of TNFRs activates the non-canonical NF-κB signaling pathway, ultimately reducing mitochondria-dependent apoptosis in OS cells [50]. The contradictory results regarding the expression of these *TNFRSF1A* genes may be related to tissue specificity and age range. Therefore, it is speculated that next step needs to be supported by a pan-cancer analysis.

In this study, we identified other potential NRGs associated with OS. *HMGB1* mainly promotes inflammation, cell differentiation, and tumor cell migration [51]. However, in contrast to *TNFRSF1A, HMGB1* is delineated as a gene associated with tumor malignancy, demonstrating the potential targeting efficacy of *HMGB1* within the immune checkpoint and tumor microenvironment [52,53]. Our study uncovers *HMGB1* as a functionally implicated gene linked to adverse prognosis in OS, potentially rendering it a target for numerous non-coding RNAs that regulate this condition [54,55]. Signal transducer and activator of transcription 3 (STAT3) is a recognized proto-oncogene, and its sustained activation is associated with the development of various cancers. In OS, elevated expression of STAT3 is linked to an adverse prognosis while driving disease processes, such as proliferation and immune evasion [56]. Wang et al. found that lncRNA AK093407 is highly expressed in both OS cells and tissues, facilitating cell proliferation and survival through STAT3 activation while inhibiting apoptosis in the OS cell line U-2OS [57]. Jiang et al. discovered that the combination of AMD3100 and triptolide effectively reduced the proliferation and metastasis of U2OS cells, while inducing apoptosis. This effect is potentially attributed to the modulation of NF-κB pathways. Egusquiaguirre et al. treated a triple-negative breast cancer (TNBC) cell line with pyrimethamine and PMPTP to block STAT3 transcription, resulting in significant downregulation of TNFRSF1A gene expression [58]. Subsequent investigations revealed that STAT3 directly interacts with the regulatory region of the TNFRSF1A gene, thereby regulating its expression level and influencing breast cancer progression through the STAT3/TNFRSF1A/NF-κB axis [59]. Currently, research on the STAT3/TNFRSF1A/NF-κB axis in OS is lacking. Substantial evidence indicates a correlation between single nucleotide polymorphisms (SNP) and OS pathogenesis. Oliveira et al. demonstrated that patients with OS harboring the GG genotype of TNF-β

rs909253 exhibited a 20% event-free survival rate at 100 mo [60]. Wang et al. found that the single nucleotide variant (SNV) TNF-α rs1800629 increased the risk of OS [61]. In contrast, Liu et al. reported no significant association between the rs1800629 polymorphism of TNF-α and OS risk [62]. The divergent findings in the aforementioned studies may be attributed to variation in sample size. Further large-scale trials are warranted to explore the issue comprehensively.

Immune infiltration analysis showed that in the *TNFRSF1A* risk group, activated dendritic cell expression levels were high in the high-expression group, and activated CD8+ T cell expression levels were high in the low-expression group. These results indicated that when TNFRSF1A expression was reduced to accelerate the OS process, CD8+ T cells were significantly activated to play a cell-killing role. Zhang et al. also found that OS progression is accompanied by a high expression of activated CD8+ T cells, which is consistent with our study [63]. Tumor cells can activate the immune checkpoint of CD8+ T cells, which prevents antigen presentation and T cell proliferation, thereby suppressing the immune function of T cells [64]. Hua et al. conducted NMF clustering analysis on various subgroups and assessed the proportions and distinctions of 22 specific immune cell types using CIBERSORT. They observed statistically significant differences in tumor microenvironment scores and CD8+ T cells among the different subgroups. However, further analyses of the immune checkpoints have not yet been conducted [15]. Immune checkpoints, clusters of molecules present on the surface of immune cells, are designed to modulate the intensity of immune activation and prevent immune overload. However, immune checkpoint inhibitors (ICIs) can unlock the self-limitation of T cells, in turn eliciting an immune response to destroy tumor cells, and are a widely accepted new-generation oncology treatment [48] Common immune checkpoints include programmed cell death protein 1 (*PD-1*), CTLA4, and LAG-3 [65] *LAG-3* is the third immune checkpoint available for cancer treatment, and in melanoma, *LAG3* in combination with PD-1, significantly improves tumor prognosis [66]. In TARGET-OS, the *LAG-3* immune checkpoint was highly expressed in samples with high TNFRSF1A expression. This indicated that *LAG-3* on the surface of T cells in the low-risk group was suppressed to prevent immune overload. In contrast, in the high-risk group, *LAG-3* expression was reduced, and T-cell suppression was enhanced to enhance immunity. Our immune score analysis also corroborated the idea that the median expres-

sion of **TNFRSF1A** distinguishes between the high- and low-risk groups. Higher tumor purity was observed in the high-risk group, whereas stromal, immune, and estimated scores were all clearly lower than those in the low-risk group.

This study had some limitations. First, as a bioinformatics analysis, this study presents a theoretical diagnostic model that has not been experimentally validated and its accuracy still needs to be evaluated. Therefore, larger sample sizes are required to verify and improve the clinical translation potential of the signature. In addition, limited genetic data are available for the analysis of immune infiltration and immune scores; therefore, heterotypic cell associations and disorders induced by various illnesses might contribute to bias in immunoassays. Finally, the relationship between the potential mechanism of **TNFRSF1A** and OS needs to be discussed in detail.

5. Conclusion

In this study, we identified **TNFRSF1A** as a critical necroptosis-based prognostic gene for OS using univariate Cox regression analysis. Immune analysis revealed the involvement of the immune checkpoint **LAG-3** in CD8+ T cells in OS pathogenesis. The consistent results obtained in the validation groups GSE16091 and GSE21257 further support the significance of **TNFRSF1A**. Notably, our findings based on the Kaplan-Meier curves and AUC analysis demonstrate that low **TNFRSF1A** expression is significantly associated with poor OS. In addition, our clinical prediction model validated the prognostic value of **TNFRSF1A**. The findings suggest that **TNFRSF1A** plays a crucial role in modulating the tumor immune microenvironment, which could guide clinical immunotherapy approaches for OS.

Acknowledgments

Author contributions

Yuke Zhang and Kai Liu contributed to the conception, design, and manuscript preparation; Jianzhong Wang contributed to the revision of important intellectual content and supervision. All authors contributed to the article and approved the submitted version.

Funding

Supplementary data

The supplementary files are available to download from http://dx.doi.org/10.3233/CBM-230086.

References

[1] M.W. Bishop, K.K. Ness, C. Li, W. Liu, D.K. Srivastava, W. Chemaitilly, K.R. Krull, D.M. Green, A.S. Pappo, L.L. Robison, M.M. Hudson and D.A. Mulrooney, Cumulative burden of chronic health conditions in adult survivors of osteosarcoma and ewing sarcoma: A report from the st. jude lifetime cohort study, *Cancer Epidemiology, Biomarkers & Prevention* **29** (2020), 1627–1638.

[2] M.F. Hansen, M. Seton and A. Merchant, Osteosarcoma in paget's disease of bone, *Journal of Bone and Mineral Research* **21** (2006), P58–P63.

[3] Y. Xu, F. Shi, Y. Zhang, M. Yin, X. Han, J. Feng and G. Wang, Twenty-year outcome of prevalence, incidence, mortality and survival rate in patients with malignant bone tumors, *International Journal of Cancer* **n/a** (2023).

[4] L. Mirabello, R.J. Troisi and S.A. Savage, Osteosarcoma incidence and survival rates from 1973 to 2004, *Cancer* **115** (2009), 1531–1543.

[5] M.A. Harris and C.J. Hawkins, Recent and ongoing research into metastatic osteosarcoma treatments, *Int J Mol Sci* **23** (2022).

[6] B. Moukengue, M. Lallier, L. Marchandet, M. Baud'huin, F. Verrecchia, B. Ory and F. Lamoureux, Origin and therapies of osteosarcoma, *Cancers (Basel)* **14** (2022).

[7] S. Miwa, N. Yamamoto, K. Hayashi, A. Takeuchi, K. Igarashi and H. Tsuchiya, Therapeutic targets for bone and soft-tissue sarcomas, *Int J Mol Sci* **20** (2019).

[8] Y.X. Ge, T.W. Zhang, L. Zhou, W. Ding, H.F. Liang, Z.C. Hu, Q. Chen, J. Dong, F.F. Xue, X.F. Yin and L.B. Jiang, Enhancement of anti-PD-1/PD-L1 immunotherapy for osteosarcoma using an intelligent autophagy-controlling metal organic framework, *Biomaterials* **282** (2022), 121407.

[9] C. Zhang and N. Liu, Ferroptosis, necroptosis, and pyroptosis in the occurrence and development of ovarian cancer, *Front Immunol* **13** (2022), 920059.

[10] J. Clusmann, K.C. Franco, D.A.C. Suárez, I. Katona, M.G. Minguez, N. Boersch, K.P. Pissas, J. Vanek, Y. Tian and S. Gründer, Acidosis induces RIPK1-dependent death of glioblastoma stem cells via acid-sensing ion channel 1a, *Cell Death Dis* **13** (2022), 702.

[11] J. Zhu, J. Wang, T. Wang, H. Zhou, M. Xu, J. Zha, C. Feng, Z. Shen, Y. Jiang and J. Chen, Identification of molecular subtypes, risk signature, and immune landscape mediated by

necroptosis-related genes in non-small cell lung cancer, *Front Oncol* **12** (2022), 955186.

[12] Y. Gong, J. Qiu, J. Ye, T. Jiang, W. Zhang, X. Zheng, Z. Zhu, L. Chen, Z. Wang, S. Mi and Z. Hong, AZ-628 delays osteoarthritis progression via inhibiting the TNF-α-induced chondrocyte necroptosis and regulating osteoclast formation, *Int Immunopharmacol* **111** (2022), 109085.

[13] X. Fan, X. Xu, X. Wu, R. Xia, F. Gao, Q. Zhang and W. Sun, The protective effect of DNA aptamer on osteonecrosis of the femoral head by alleviating TNF-α-mediated necroptosis via RIP1/RIP3/MLKL pathway, *J Orthop Translat* **36** (2022), 44–51.

[14] J. Li, X. Tang, Y. Du, J. Dong, Z. Zhao, H. Hu, T. Song, J. Guo, Y. Wang, T. Xu, C. Shao, Y. Sheng and Y. Xi, Establishment of an autophagy-related clinical prognosis model for predicting the overall survival of osteosarcoma, *Biomed Res Int* **2021** (2021), 5428425.

[15] L. Hua, P. Lei and Y. Hu, Construction and validation model of necroptosis-related gene signature associates with immunity for osteosarcoma patients, *Sci Rep* **12** (2022), 15893.

[16] Y. Zheng, J. Xu, J. Lin and Y. Lin, A Novel Necroptosis-Related lncRNA Signature for Osteosarcoma, *Comput Math Methods Med* **2022** (2022), 8003525.

[17] S. Boboila, G. Lopez, J. Yu, D. Banerjee, A. Kadenhe-Chiweshe, E.P. Connolly, J.J. Kandel, P. Rajbhandari, J.M. Silva, A. Califano and D.J. Yamashiro, Transcription factor activating protein 4 is synthetically lethal and a master regulator of MYCN-amplified neuroblastoma, *Oncogene* **37** (2018), 5451–5465.

[18] Y. Shi, R. He, Z. Zhuang, J. Ren, Z. Wang, Y. Liu, J. Wu, S. Jiang and K. Wang, A risk signature-based on metastasis-associated genes to predict survival of patients with osteosarcoma, *J Cell Biochem* **121** (2020), 3479–3490.

[19] M. Yang, X. Ma, Z. Wang, T. Zhang, Y. Hua and Z. Cai, Identification of a novel glycolysis-related gene signature for predicting the prognosis of osteosarcoma patients, *Aging (Albany NY)* **13** (2021), 12896–12918.

[20] T. Barrett, D.B. Troup, S.E. Wilhite, P. Ledoux, D. Rudnev, C. Evangelista, I.F. Kim, A. Soboleva, M. Tomashevsky and R. Edgar, NCBI GEO: Mining tens of millions of expression profiles-database and tools update, *Nucleic Acids Res* **35** (2007), D760–5.

[21] M.E. Ritchie, B. Phipson, D. Wu, Y. Hu, C.W. Law, W. Shi and G.K. Smyth, limma powers differential expression analyses for RNA-sequencing and microarray studies, *Nucleic Acids Res* **43** (2015), e47.

[22] N. Wang and D. Liu, Identification and validation a necroptosis-related prognostic signature and associated regulatory axis in stomach adenocarcinoma, *Onco Targets Ther* **14** (2021), 5373–5383.

[23] J.C. Xi, H.Y. Zang, L.X. Guo, H.B. Xue, X.D. Liu, Y.B. Bai and Y.Z. Ma, The PI3K/AKT cell signaling pathway is involved in regulation of osteoporosis, *J Recept Signal Transduct Res* **35** (2015), 640–645.

[24] L. Xiang, W. Yang, F. Wang and G. Liu, Circ_0083964 knockdown impedes rheumatoid arthritis progression via the miR-204-5p-dependent regulation of YY1, *J Orthop Surg Res* **17** (2022), 558.

[25] M. Ashburner, C.A. Ball, J.A. Blake, D. Botstein, H. Butler, J.M. Cherry, A.P. Davis, K. Dolinski, S.S. Dwight, J.T. Eppig, M.A. Harris, D.P. Hill, L. Issel-Tarver, A. Kasarskis, S. Lewis, J.C. Matese, J.E. Richardson, M. Ringwald, G.M. Rubin and G. Sherlock, Gene ontology: Tool for the unification of biology. The Gene Ontology Consortium, *Nat Genet* **25** (2000), 25–29.

[26] M. Kanehisa and S. Goto, KEGG: Kyoto encyclopedia of genes and genomes, *Nucleic Acids Res* **28** (2000), 27–30.

[27] G. Yu, L.G. Wang, Y. Han and Q.Y. He, clusterProfiler: An R package for comparing biological themes among gene clusters, *Omics* **16** (2012), 284–287.

[28] T. Wu, E. Hu, S. Xu, M. Chen, P. Guo, Z. Dai, T. Feng, L. Zhou, W. Tang, L. Zhan, X. Fu, S. Liu, X. Bo and G. Yu, clusterProfiler 4.0: A universal enrichment tool for interpreting omics data, *Innovation (Camb)* **2** (2021), 100141.

[29] W. Walter, F. Sánchez-Cabo and M. Ricote, GOplot: An R package for visually combining expression data with functional analysis, *Bioinformatics* **31** (2015), 2912–2914.

[30] A. Subramanian, P. Tamayo, V.K. Mootha, S. Mukherjee, B.L. Ebert, M.A. Gillette, A. Paulovich, S.L. Pomeroy, T.R. Golub, E.S. Lander and J.P. Mesirov, Gene set enrichment analysis: A knowledge-based approach for interpreting genome-wide expression profiles, *Proc Natl Acad Sci U S A* **102** (2005), 15545–15550.

[31] A. Liberzon, C. Birger, H. Thorvaldsdóttir, M. Ghandi, J.P. Mesirov and P. Tamayo, The Molecular Signatures Database (MSigDB) hallmark gene set collection, *Cell Syst* **1** (2015), 417–425.

[32] C. von Mering, M. Huynen, D. Jaeggi, S. Schmidt, P. Bork and B. Snel, STRING: A database of predicted functional associations between proteins, *Nucleic Acids Res* **31** (2003), 258–261.

[33] P. Charoentong, F. Finotello, M. Angelova, C. Mayer, M. Efremova, D. Rieder, H. Hackl and Z. Trajanoski, Pan-cancer immunogenomic analyses reveal genotype-immunophenotype relationships and predictors of response to checkpoint blockade, *Cell Rep* **18** (2017), 248–262.

[34] S. Bhattacharya, P. Dunn, C.G. Thomas, B. Smith, H. Schaefer, J. Chen, Z. Hu, K.A. Zalocusky, R.D. Shankar, S.S. Shen-Orr, E. Thomson, J. Wiser and A.J. Butte, ImmPort, toward repurposing of open access immunological assay data for translational and clinical research, *Sci Data* **5** (2018), 180015.

[35] S. Hänzelmann, R. Castelo and J. Guinney, GSVA: Gene set variation analysis for microarray and RNA-seq data, *BMC Bioinformatics* **14** (2013), 7.

[36] A. Kalbasi and A. Ribas, Tumour-intrinsic resistance to immune checkpoint blockade, *Nat Rev Immunol* **20** (2020), 25–39.

[37] K. Yoshihara, M. Shahmoradgoli, E. Martínez, R. Vegesna, H. Kim, W. Torres-Garcia, V. Treviño, H. Shen, P.W. Laird, D.A. Levine, S.L. Carter, G. Getz, K. Stemke-Hale, G.B. Mills and R.G. Verhaak, Inferring tumour purity and stromal and immune cell admixture from expression data, *Nat Commun* **4** (2013), 2612.

[38] X. Wu, S. Qiao, W. Wang, Y. Zhang, J. Shi, X. Zhang, W. Gu, X. Zhang, Y. Li, X. Ding, J. Wei, Y. Gu and H. Lai, Melatonin prevents peri-implantitis via suppression of TLR4/NF-κB, *Acta Biomater* **134** (2021), 325–336.

[39] Y. Zhu, B. Chang, Y. Pang, H. Wang and Y. Zhou, Advances in Hypoxia-Inducible Factor-1α Stabilizer Deferoxamine in Tissue Engineering, Tissue Eng Part B Rev, 2023.

[40] J. Cheng, X. Duan, X. Fu, Y. Jiang, P. Yang, C. Cao, Q. Li, J. Zhang, X. Hu, X. Zhang and Y. Ao, RIP1 perturbation induces chondrocyte necroptosis and promotes osteoarthritis pathogenesis via targeting BMP7, *Front Cell Dev Biol* **9** (2021), 638382.

[41] B. He, Y. Zhu, H. Cui, B. Sun, T. Su and P. Wen, Comparison of Necroptosis With Apoptosis for OVX-Induced Osteoporosis, *Front Mol Biosci* **8** (2021), 790613.

[42] X. Liu, F. Lu and X. Chen, Examination of the role of necrop-

totic damage-associated molecular patterns in tissue fibrosis, *Front Immunol* **13** (2022), 886374.

[43] T. Akagi, S. Hiramatsu-Asano, K. Ikeda, H. Hirano, S. Tsuji, A. Yahagi, M. Iseki, M. Matsuyama, T.W. Mak, K. Nakano, K. Ishihara, Y. Morita and T. Mukai, TRAPS mutations in Tnfrsf1a decrease the responsiveness to TNFα via reduced cell surface expression of TNFR1, *Front Immunol* **13** (2022), 926175.

[44] J. Dai and Y. Fu, Identification of necroptosis-related gene signature and characterization of tumour microenvironment infiltration in non-small-cell lung cancer, *J Cell Mol Med* **26** (2022), 4698–4709.

[45] S. Xin, J. Mao, C. Duan, J. Wang, Y. Lu, J. Yang, J. Hu, X. Liu, W. Guan, T. Wang, S. Wang, J. Liu, W. Song and X. Song, Identification and quantification of necroptosis landscape on therapy and prognosis in kidney renal clear cell carcinoma, *Front Genet* **13** (2022), 832046.

[46] Z. Li, C. Jin, X. Lu, Y. Zhang, Y. Zhang, J. Wen, Y. Liu, X. Liu and J. Li, Developing a 5-gene signature related to pyroptosis for osteosarcoma patients, *J Oncol* **2022** (2022), 1317990.

[47] J. Bolik, F. Krause, M. Stevanovic, M. Gandraß, I. Thomsen, S.S. Schacht, E. Rieser, M. Müller, N. Schumacher, J. Fritsch, R. Wichert, E. Galun, J. Bergmann, C. Röder, C. Schafmayer, J.H. Egberts, C. Becker-Pauly, P. Saftig, R. Lucius, W. Schneider-Brachert, R. Barikbin, D. Adam, M. Voss, W. Hitzl, A. Krüger, B. Strilic, I. Sagi, H. Walczak, S. Rose-John and D. Schmidt-Arras, Inhibition of ADAM17 impairs endothelial cell necroptosis and blocks metastasis, *J Exp Med* **219** (2022).

[48] M.M. Speeckaert, R. Speeckaert, M. Laute, R. Vanholder and J.R. Delanghe, Tumor necrosis factor receptors: Biology and therapeutic potential in kidney diseases, *Am J Nephrol* **36** (2012), 261–270.

[49] E.M. Meškytė, L. Pezzè, L. Bartolomei, M. Forcato, I.A. Bocci, G. Bertalot, M. Barbareschi, L. Oliveira-Ferrer, A. Bisio, S. Bicciato, D. Baltriukienė and Y. Ciribilli, ETV7 reduces inflammatory responses in breast cancer cells by repressing the TNFR1/NF-κB axis, *Cell Death Dis* **14** (2023), 263.

[50] S. Lin, L. Zhou, Y. Dong, Q. Yang, Q. Yang, H. Jin, T. Yuan and S. Zhou, Alpha-(16)-fucosyltransferase, (FUT8) affects the survival strategy of osteosarcoma by remodeling TNF/NF-κB2 signaling, *Cell Death Dis* **12** (2021), 1124.

[51] F. Novelli, A. Bononi, Q. Wang, F. Bai, S. Patergnani, F. Kricek, E. Haglund, J.S. Suarez, M. Tanji, R. Xu, Y. Takanishi, M. Minaai, S. Pastorino, P. Morris, G. Sakamoto, H.I. Pass, G. Barbour, G. Gaudino, C. Giorgi, P. Pinton, J.N. Onuchic, H. Yang and M. Carbone, BAP1 forms a trimer with HMGB1 and HDAC1 that modulates gene × environment interaction with asbestos, *Proc Natl Acad Sci U S A* **118** (2021).

[52] P. Hubert, P. Roncarati, S. Demoulin, C. Pilard, M. Ancion, C. Reynders, T. Lerho, D. Bruyere, A. Lebeau, C. Radermecker, M. Meunier, M.J. Nokin, E. Hendrick, O. Peulen, P. Delvenne and M. Herfs, Extracellular HMGB1 blockade inhibits tumor growth through profoundly remodeling immune microenvironment and enhances checkpoint inhibitor-based immunotherapy, *J Immunother Cancer* **9** (2021).

[53] Y. Ren, L. Cao, L. Wang, S. Zheng, Q. Zhang, X. Guo, X. Li, M. Chen, X. Wu, F. Furlong, Z. Meng and K. Xu, Autophagic secretion of HMGB1 from cancer-associated fibroblasts promotes metastatic potential of non-small cell lung cancer cells via NFκB signaling, *Cell Death Dis* **12** (2021), 858.

[54] P. Lou, T. Ding and X. Zhan, Long Noncoding RNA HNF1A-AS1 Regulates Osteosarcoma Advancement Through Modulating the miR-32-5p/HMGB1 Axis, *Cancer Biother Radiopharm* **36** (2021), 371–381.

[55] Y. Yu, G. Dong, Z. Li, Y. Zheng, Z. Shi and G. Wang, circ-LRP6 contributes to osteosarcoma progression by regulating the miR-141-3p/HDAC4/HMGB1 axis, *Int J Oncol* **60** (2022).

[56] Y. Liu, S. Liao, S. Bennett, H. Tang, D. Song, D. Wood, X. Zhan and J. Xu, STAT3 and its targeting inhibitors in osteosarcoma, *Cell Prolif* **54** (2021), e12974.

[57] Long non-coding RNA AK093407 promotes proliferation and inhibits apoptosis of human osteosarcoma cells via STAT3 activation [Retraction], *Am J Cancer Res* **11** (2021), 623.

[58] C. Jiang, X. Fang, H. Zhang, X. Wang, M. Li, W. Jiang, F. Tian, L. Zhu and Z. Bian, AMD3100 combined with triptolide inhibit proliferation, invasion and metastasis and induce apoptosis of human U2OS osteosarcoma cells, *Biomed Pharmacother* **86** (2017), 677–685.

[59] S.P. Egusquiaguirre, J.E. Yeh, S.R. Walker, S. Liu and D.A. Frank, The STAT3 Target Gene TNFRSF1A Modulates the NF-κB Pathway in Breast Cancer Cells, *Neoplasia* **20** (2018), 489–498.

[60] I.D. Oliveira, A.S. Petrilli, M.H. Tavela, M.A. Zago and S.R. de Toledo, TNF-alpha, TNF-beta, IL-6, IL-10, PECAM-1 and the MPO inflammatory gene polymorphisms in osteosarcoma, *J Pediatr Hematol Oncol* **29** (2007), 293–297.

[61] X. Wang and Z. Liu, Systematic meta-analysis of genetic variants associated with osteosarcoma susceptibility, *Medicine (Baltimore)* **97** (2018), e12525.

[62] J. Liu, J. Wang, W. Jiang and Y. Tang, Effect of cytotoxic T-lymphocyte antigen-4, TNF-alpha polymorphisms on osteosarcoma: Evidences from a meta-analysis, *Chin J Cancer Res* **25** (2013), 671–678.

[63] J.A. Ligon, W. Choi, G. Cojocaru, W. Fu, E.H. Hsiue, T.F. Oke, N. Siegel, M.H. Fong, B. Ladle, C.A. Pratilas, C.D. Morris, A. Levin, D.S. Rhee, C.F. Meyer, A.J. Tam, R. Blosser, E.D. Thompson, A. Suru, D. McConkey, F. Housseau, R. Anders, D.M. Pardoll and N. Llosa, Pathways of immune exclusion in metastatic osteosarcoma are associated with inferior patient outcomes, *J Immunother Cancer* **9** (2021).

[64] M. Gupta, K. Chandan and M. Sarwat, Natural products and their derivatives as immune check point inhibitors: Targeting cytokine/chemokine signalling in cancer, *Semin Cancer Biol* **86** (2022), 214–232.

[65] S.R. Woo, M.E. Turnis, M.V. Goldberg, J. Bankoti, M. Selby, C.J. Nirschl, M.L. Bettini, D.M. Gravano, P. Vogel, C.L. Liu, S. Tangsombatvisit, J.F. Grosso, G. Netto, M.P. Smeltzer, A. Chaux, P.J. Utz, C.J. Workman, D.M. Pardoll, A.J. Korman, C.G. Drake and D.A. Vignali, Immune inhibitory molecules LAG-3 and PD-1 synergistically regulate T-cell function to promote tumoral immune escape, *Cancer Res* **72** (2012), 917–927.

[66] H.A. Tawbi, D. Schadendorf, E.J. Lipson, P.A. Ascierto, L. Matamala, E. Castillo Gutiérrez, P. Rutkowski, H.J. Gogas, C.D. Lao, J.J. De Menezes, S. Dalle, A. Arance, J.J. Grob, S. Srivastava, M. Abaskharoun, M. Hamilton, S. Keidel, K.L. Simonsen, A.M. Sobiesk, B. Li, F.S. Hodi and G.V. Long, Relatlimab and Nivolumab versus Nivolumab in Untreated Advanced Melanoma, *N Engl J Med* **386** (2022), 24–34.